

Title	Atomic-scale simulation of ALD chemistry
Authors	Elliott, Simon D.
Publication date	2012-06-22
Original Citation	ELLIOTT, S. E. 2012. Atomic-scale simulation of ALD chemistry. Semiconductor Science and Technology, 27, 074008. http://dx.doi.org/10.1088/0268-1242/27/7/074008
Type of publication	Article (peer-reviewed)
Link to publisher's version	http://stacks.iop.org/0268-1242/27/i=7/a=074008 - 10.1088/0268-1242/27/7/074008
Rights	© 2012 IOP Publishing Ltd. This is an author-created, un-copyedited version of an article published in Semiconductor Science and Technology. IOP Publishing Ltd is not responsible for any errors or omissions in this version of the manuscript or any version derived from it. The Version of Record is available online at http://dx.doi.org/10.1088/0268-1242/27/7/074008
Download date	2024-05-21 09:25:31
Item downloaded from	https://hdl.handle.net/10468/2478

Atomic scale simulation of ALD chemistry

Simon D. Elliott

Tyndall National Institute, University College Cork, Dyke Parade, Cork, Ireland

Email: simon.elliott@tyndall.ie

Telephone: +353-21-4904392

Abstract

Published papers on atomic-scale simulation of the atomic layer deposition (ALD) process are reviewed. The main topic is reaction mechanism, considering the elementary steps of precursor adsorption, ligand elimination and film densification, as well as reactions with substrates (particularly Si and SiO₂) and CVD-like decomposition at the surface. Density functional theory (DFT) is the first principles method generally applied to these mechanistic questions. Analytical and stochastic models for growth rate and growth mode are also presented, some of which incorporate atomic-scale data. The most popular subject for modeling is the ALD of oxides and nitrides, particularly the high-*k* dielectrics HfO₂, ZrO₂ and Al₂O₃, due to their importance in semiconductor processing.

PACS: 68.43.-h, 68.43.Bc, 81.15.Aa, 81.15.Gh, 82.30.-b, 82.33.Ya

1. Introduction

Simulations provide a bridge between theory and experiment, exploiting the extraordinary computational power available today so as to carry out virtual experiments and test theories in complex scenarios. This paper reviews how simulations have been brought to bear on the pulsed version of chemical vapour deposition (CVD) that is commonly called atomic layer deposition (ALD), and historically also atomic layer epitaxy. The review only covers atomic-scale simulations of the ALD reactions, and not properties of the materials deposited by ALD, nor larger-scale

simulations of film growth or gas flow. Computational studies of non-pulsed CVD and of crystal growth [1] are out of scope, as are surface science simulations that do not make conclusions specific to ALD. For instance, although ALD has many parallels with heterogeneous catalysis, the huge body of modeling work in that field [2] cannot be covered in this short review.

The role of a simulation within a scientific investigation can simply be to *validate* a model by showing agreement with experiment (and without validation a model is merely a sophisticated hypothesis). It is better if a simulation can *explain* an experimental result by providing evidence for one model over another. Best of all is if a simulation can *predict* results, narrow down experimental options and lead directly to new insights without experimental input – but of course such prediction requires a quantitative accuracy that can rarely be achieved. Nevertheless, whatever the balance between computed and measured data, computational studies can be an efficient way to investigate novel processes and shorten process development times in the laboratory.

In terms of subject matter and popularity, ALD simulations follow the same trend as ALD experiments, with most recent work motivated by the needs of the electronics industry, particularly the ALD of high-permittivity (“high- k ”) dielectrics onto semiconductors as part of the gate stack in CMOS transistors. Most of this review therefore covers the ALD of high- k oxides, both the reaction mechanisms themselves and how deposition takes place on semiconductor substrates (‘heterodeposition’). Simulations of ALD chemistry for other materials such as nitrides, sulfides and metals are also considered. A separate section reviews papers on the simulation of precursor stability.

2. Methods of atomic-scale simulation

Atomistic calculations, in which discrete atoms have explicit locations in space, are now established as an important adjunct to experiment [3]. The electronic structure is determined by approximately solving the quantum mechanical Schrödinger equation, which yields the wavefunction, energy, gradients *etc.*, and hence gives access to atomic structure, reaction energetics at zero temperature and dynamics at finite temperatures. The more accurate the approximate solution, the more demanding the computational load and the smaller the system that can be simulated. The various methods of atomistic simulation thus form a hierarchy of accuracy *versus* cost and system size. Of these, first

principles (or *ab initio*) methods are distinguished by requiring no empirical fitting parameters, so that genuinely novel situations can be investigated.

2.1. First principles methods

Hartree Fock (HF) theory is the original *ab initio* technique, but today density functional theory (DFT) provides a higher level of accuracy at roughly the same computational cost [4],[5]. There is in fact a range of DFT approaches to approximately solving the electronic problem, but in this review we use the term ‘DFT’ as short-hand for Kohn-Sham calculations of the ground state using the local density approximation or generalized gradient approximation, often mixed with HF exchange (hybrid DFT). Physically, the trick in these DFT calculations is to find the density of mutually-interacting electrons by computing non-interacting pseudo-electrons subject to a potential that partially accounts for electron correlation and exchange.

DFT generally gives a good description of classical two-centre covalent bonds, non-classical multi-centre bonds, metallic bonding in conductors, and polar/ionic bonding in semiconductors and insulators. However, ‘self-interaction’ in the DFT density means that there are systematic but unpredictable errors in band gaps, defect levels, excited state properties, van der Waals (dispersion) interactions and curve-crossing at transition states. For ALD, this means that DFT is highly accurate in determining changes in structure and bonding when organometallic molecules interact with various material surfaces, *i.e.* reaction mechanism, and an overview of these studies is given in Table 1. Computed properties such as vibrational spectra can help in the assignment of experimental data and thus provide direct evidence for mechanism [6],[7],[8]. On the other hand, volatility is difficult to simulate with DFT, because of the poor description of weak inter-molecular forces. One approach is to compute the energetics of oligomerisation, as has been pursued for variously-substituted imidazolate ligands of strontium [9]. There is also an upper limit on the system size that can be simulated with DFT, although algorithmic and hardware advances mean that this limit is being pushed ever upwards: today, DFT is the method of choice for systems of 100-1000 atoms, occupying roughly one cubic nanometer.

The main source of uncertainty in first principles calculations is therefore the choice of model and its interpretation. This review will include a brief assessment of various models for describing ALD. The proposed model should be viewed as a hypothesis and the first principles simulation ensures that accurate structures and energies can be obtained for this hypothesis, without fitting to experiment.

2.2. Activation energies

It is commonly stated that ALD is driven by kinetics, rather than thermodynamics, appealing presumably to the irreversible loss of by-products into the stream of exhaust gases. One could argue that certain reaction steps are reversible and thermodynamically controlled, such as the sampling of surface sites by frequently adsorbing/desorbing precursor molecules, and the densification of ad-layers to match the contour of the substrate. Nevertheless, the competition between slower side-reactions and faster growth reactions is crucial for successful ALD, and hence much of the focus of atomic-scale simulations is on the activation energies for such reaction steps.

Computing Gibbs free energies of activation to so-called ‘chemical accuracy’ ($<5 \text{ kJ.mol}^{-1}$) remains an embarrassing difficulty in atomic-scale simulation [5]. Such bond-making/-breaking can only sensibly be attempted with *ab initio* methods (*e.g.* HF or approximate DFT), thereby limiting the system size to <1000 atoms on today’s computer hardware. Even so, error cancellation is poor when the wavefunction changes strongly at the transition state, so that chemical accuracy can only reliably be achieved by post-HF methods such as coupled cluster [10],[11] or configuration interaction [12], tractable for fewer than 100 atoms.

There is therefore an unavoidable trade-off between the accuracy of the quantum mechanical solution and the veracity of the atomic model. The latter depends on the number of atoms, the number of possible geometries, and how many alternative pathways can be tested. For example, if the model contains just one H and one ligand, then the number of possible H-transfer pathways is clearly unrealistically low compared to actual ligands on an OH-covered surface. In this sense, ergodicity (*i.e.* whether all relevant pathways can be sampled) is as big a problem as accuracy when computing activation energies. In principle, all that is needed to sample more pathways with higher accuracy is computational brute force, which is now available in massively-parallel computers. However

practical experience shows that ALD chemistries are so complicated that automated searches are rarely successful, and that the bias of the user in defining models is still a major constraint.

Table 1: Overview of primary studies of ALD via atomic-scale (mostly DFT) simulation, ordered alphabetically by precursor formula.

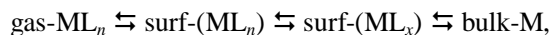
Precursors	Product film	Reference
$\text{AlCl}_3 + \text{H}_2\text{O}$	Al_2O_3	[12] , [13]
$\text{AlMe}_3 + \text{H}_2\text{O}$	Al_2O_3	[14], [15], [16], [17], [18], [19], [20], [21], [22], [23], [24], [25], [26], [27], [28], [29], [30], [31], [32], [33], [34], [35], [36], [37]
$\text{AlMe}_3 + \text{O}_3$	Al_2O_3	[38], [39]
$\text{AlMe}_2(\text{O}^i\text{Pr})$	Al_2O_3	[40]
$\text{BH}_3\text{or BBr}_3 + \text{NH}_3$	BN	[41]
$\text{B}(\text{OMe})_3 + \text{POCl}_3$	BPO_4	[42]
CF_3R	C	[43]
$\text{CdMe}_2 + \text{H}_2\text{S}$	CdS	[44]
$\text{Co}(\text{allyl})(\text{CO})_3$	Co	[45]
$\text{Co}(\text{amd})$	Co	[46], [47]
$[\text{Cu}(\text{amd})]_2 + \text{H}_2$	Cu	[48]
$\text{Cu}(\beta\text{-diketonate})_2$	Cu	[49]
$\text{Cu}_2\text{Cl}_2 + \text{H}_2$	Cu	[50], [51], [52]
$\text{Cu}(\text{hfac})(\text{vtms})$	Cu	[53], [54], [55]
$[\text{Cu}(\text{N}^i\text{Pr})_2\text{CNMe}_2]_2$	Cu	[56]
$\text{ErCp}_3 + \text{O}_3$	Er_2O_3	[57]
$\text{GaCl}_3 + \text{H}_2$	GaAs	[58]
$\text{HfCl}_4 + \text{H}_2\text{O}$	HfO_2	[22], [23], [59], [60], [61], [62], [63], [64], [65], [36]
$\text{Hf}(\text{Cp}_2\text{CMe}_2)_2 + \text{O}_3$, $\text{Hf}(\text{Cp}_2\text{CMe}_2)(\text{Me})(\text{OMe}) + \text{O}_3$	HfO_2	[66]
$\text{Hf}(\text{NEtMe})_4$	HfO_2	[67]
$\text{Hf}(\text{NMe}_2)_4 + \text{NH}_3$	HfN , HfO_2	[68], [69]
$\text{HfX}_4 + \text{H}_2\text{O}$	HfO_2	[70]
$\text{La}(\text{amd})_3 + \text{O}_3$	La_2O_3	[6]
$\text{LaCp}_3 + \text{O}_3$	La_2O_3	[57]
$\text{LaX}_3 + \text{O}_3$	La_2O_3	[71]
$\text{Mg}(\text{C}_5\text{H}_5)_2 + \text{H}_2\text{O}$	MgO	[72]
$\text{Mo}(\text{tBuN})_2(\text{NR}_2)_2$	MoN	[73]
NH_3	nitrides	[74]
$\text{Ni}(\text{amd})$	Ni	[46], [47]
$\text{Pb}(\text{thd})_2 + \text{H}_2\text{S}$	PbS	[75]
$\text{SiCl}_4 + \text{H}_2\text{O}$, SiCl_xH_y	SiO_2	[76], [77], [78]
$\text{SiH}_4 + \text{NH}_3$	Si_3N_4	[79]
$\text{Si}(\text{OMe})_4 + \text{HfCl}_4$	HfSiO_x	[80],[81]
$\text{SnX}_4 + \text{H}_2\text{O}$	SnO_2	[70]
$\text{Sr}(\text{RCp})_2$	SrO , SrTiO_3	[82]
$\text{Sr}(\beta\text{-diketonate})_2$	SrO , SrTiO_3	[82]
$\text{Sr}(\text{imid})_2$	SrO , SrTiO_3	[9]
$\text{TaCl}_5 + \text{H}_2\text{O}$	Ta_2O_5	[10]
$\text{Ta}(\text{NMe}_2)_5 + \text{H}_2\text{-plasma}$	TaN, TaCN	[69], [83]

$\text{Ta}(\text{tBuN})(\text{NEt}_2)_3 + \text{NH}_3$	TaN	[84]
$\text{TiCp}_2((\text{N}^i\text{Pr})_2\text{CN}(\text{H})^i\text{Pr})$	TiN, TiO_2 , SrTiO_3	[85]
$\text{Ti}(\text{CpMe}_5)(\text{OMe})_3 + \text{H}_2\text{O}$	TiO_2	[86], [87]
TiCl_4	TiO_2 , TiN	[88], [89], [90], [91]
$\text{TiI}_4 + \text{H}_2\text{O}$	TiO_2	[92]
$\text{Ti}(\text{NMe}_2)_4$	TiN, TiZrN, TiO_2 , SrTiO_3	[69], [93], [94], [95]
$\text{Ti}(\text{O}^i\text{Pr})_4 + \text{H}_2\text{O}$	TiO_2	[93]
$\text{W}(\text{Me}_3\text{CN})_2(\text{NMe}_2)_2$	WN, WCN	[69]
$\text{Zn}(\text{C}_2\text{H}_5)_2 + \text{H}_2\text{O}$	ZnO	[96]
$\text{ZrCl}_4 + \text{H}_2\text{O}$	ZrO_2	[97], [98], [99], [100], [101], [102], [103], [104], [22], [65]
$\text{Zr}(\text{Cp}_2\text{CMe}_2)\text{Me}_2 + \text{O}_3$, $\text{Zr}(\text{Cp}_2\text{CMe}_2)(\text{Me})(\text{OMe}) + \text{O}_3$	ZrO_2	[66]
$\text{Zr}(\text{Cp})_2(\text{Me})_2$	ZrO_2	[105], [106]
$\text{Zr}(\text{MeCp})_2(\text{Me})(\text{OMe})$	ZrO_2	[107]
$\text{Zr}(\text{NMe}_2)_4$	ZrO_2 , TiZrN	[69], [108]
$\text{YCp}_3 + \text{H}_2\text{O}$	Y_2O_3	[109]

3. Simulating reaction mechanism during homodeposition

Unlike standard CVD, the steady state during a single ALD pulse is when the surface is saturated and no further net reaction occurs. Instead, ‘steady-state’ is used here to refer to the constant growth rate that is achieved over cycles of product-on-product growth, which we may also term ‘homodeposition’ in order to distinguish it from the initial product-on-substrate cycles. ALD process development is clearly dependent on understanding first the mechanism of homodeposition, and after that, the mechanism of deposition onto various substrates (section 4). The aim is to identify the elementary chemical reactions that transform precursor molecules into product films (both ALD and non-ALD reactions), as well as those that lead to undesired by-products or impurities. This knowledge should enable us to answer the key questions about a particular ALD process, namely, how does the surface become saturated in one pulse and how are these groups consumed during the next pulse? Quantitative answers to these questions yield predictions of growth rate, temperature dependence and pulse/purge durations, and help in choosing ligands and designing processes for new materials. As shown in the following sections, many simulations have achieved these goals.

In ideal ALD, precursors react only on the growing surface and not in the gas-phase. The film growth reactions of a precursor for element M may therefore be written:

Equation 1

where ML_n is a metal-containing precursor with n ligands L , ligands can be eliminated from the surface so that $0 \leq x \leq n$, and ‘bulk-M’ refers to the an atom in a local environment like that of the as-deposited solid film. The position of the equilibria between the steps in Equation 1 depends on the reaction energetics and on the availability of reagents and ligands during the pulse-purge cycle of ALD. The first step is molecular adsorption. The second step shows the nature of adsorption changing as ligands are eliminated. The final ‘bulk’ status may not be reached until after many ALD cycles. In a general sense, the whole sequence in Equation 1 is the reactive adsorption of a precursor onto the surface, along with the desorption of ligand remnants. Describing the ALD reaction mechanism means describing each of the steps in Equation 1, and in particular, describing the various interactions between ML_x adsorbates and the substrate or growing surface.

Adsorption of the precursor molecule onto a substrate is the first stage in the chemical reactions of deposition. There are numerous first principles computational studies of adsorption, both of organometallic complexes and of molecules like H_2O , NH_3 and O_2 that are used as co-reagents in ALD, and it is not possible to review all these studies here. This survey is instead limited to papers where computation of reaction steps leads to a conclusion about the mechanism of ALD (Table 1). As will be seen, most of these studies do consider molecular adsorption of organometallic precursor or co-reagent, and also the subsequent elimination of ligands.

3.1. Mechanism of oxide ALD

For the mechanism of oxide ALD, possibly the earliest quantum chemical study is that by Siodmiak, Frenking and Korkin on $\text{TaCl}_5 + \text{H}_2\text{O}$ [10]. The model consists of complexes totalling ten atoms or less, and despite the model being so small, reasonable reaction energies are obtained for adsorption, HCl elimination and etching. Energy barriers for intra-ligand reaction pathways are also computed, even though these pathways are highly constrained relative to an actual surface.

The next mechanism to be computed with DFT was the prototypical ALD system $\text{AlMe}_3 + \text{H}_2\text{O}$ ($\text{Me} = \text{CH}_3$) by Widjaja and Musgrave [14]. An Al_2 cluster model is used and tested against an Al_4

cluster (up to 30 atoms), showing little non-local electronic effect on the reactions. Adsorption of AlMe_3 onto a surface hydroxyl group is found to form a Lewis acid-base adduct and a barrier was found for intra-cluster proton transfer producing CH_4 . Calculations yield a similar energy profile for the corresponding H_2O half-reactions. A similar model is used to determine activation energies for kinetics, which are fed into continuum simulation of alumina ALD [19].

Widjaja and Musgrave follow a similar approach based on Hf_4 or Hf_8 clusters in their early study of HfO_2 from metal-chloride precursors and H_2O [60]. In both half-reactions, the zero-temperature energetics show strongly-favoured adsorption of the precursor molecule, but a barrier and overall energy cost for subsequent elimination of HCl , confirmed later in a periodic model.[61] Inclusion of entropy effects at realistic ALD temperatures turns out to be decisive – reducing the adsorption free energy and making desorption of HCl more favourable, albeit still via a substantial barrier. The results for ZrCl_4 are nearly identical [97]. Similar results are obtained for AlCl_3 , along with consideration of a non-growth side-reaction [12]. Hydroxychloride side-products are also computed [13]. Since growth is a multi-step reaction in competition with side-reactions, it is not straightforward to correlate the computed energy minima and barriers with the experimental growth rate (*e.g.* the trend with increasing temperature). Nevertheless, this case illustrates that endothermic reaction steps are not necessarily an obstacle to film growth in ALD, presumably because certain reaction steps are far from chemical equilibrium. Calculating the activation and reaction energies for a single pathway has therefore no predictive power on its own.

The coverage-dependence of water adsorption and surface acidity is added to the picture in cluster calculations by Deminsky *et al.* [100] (confirmed later in a periodic model [101]) and the authors note that “the mechanism and kinetics of the ALD process cannot be interpreted even qualitatively without taking into account stereochemical effects, in particular, the effects of surface coverage on the reactivity of chemisorbed surface species.”

The $\text{AlMe}_3+\text{H}_2\text{O}$ mechanism is investigated by Elliott and Greer using a periodic model [15]. The model imposes crystallinity and so the most stable surface of the most stable crystalline polymorph of alumina is chosen as the substrate. However amorphous alumina is grown in ALD, which exhibits lower coordination numbers and it has not yet been proven whether the use of a crystalline model

negatively affects the simulation results. The energy obtained for Lewis adduct formation agrees with that from the cluster model [14] but, from the various pathways investigated, proton transfer is found to occur most readily from a neighboring hydroxyl group. Substantial release of energy is seen to accompany increases in Al-O coordination at the surface as the CH₄ by-product desorbs, in contrast to the reluctance of HCl to desorb in the cases above.

An alternative alumina process is AlMe₃+O₃, which is perhaps a model reaction for other ALD reactions with O₃ or O₂-plasma, but the reaction mechanism is much more complex. *Ab initio* molecular dynamics show that O radicals insert into metal-ligand bonds, ultimately transforming Al-CH₃ into Al-OH [38]. However, formate intermediates are detected with *in situ* IR, as confirmed by DFT assignments of the bands [39]. DFT-assigned spectra are also used to identify decomposition products for La(amd)₃+O₃ [6]. Extensive computations of surface intermediates during homodeposition from LaCp₃ and ErCp₃ (Cp=C₅H₅) are relevant for the corresponding oxide ALD processes with O₃ [57]. The La precursor is found to undergo surface-catalysed decomposition whereas C₅H₆ elimination is favoured for Er, partly due to the level of distortion in the oxide substrates, and this explains why Er₂O₃ growth is successful but La₂O₃ is not.

Sulfides have many similarities with oxides and so similar adsorption and elimination reactions are computed for CdS homodeposition from CdMe₂+H₂S.[44] The calculated reaction barriers for the ALD half reactions suggest that elevated temperatures are required for the film growth.

Once reaction mechanism and associated kinetics are understood, modelling can also help in the design of improved processes. For instance, a DFT study of the effect of various Lewis bases in catalysing the ALD of SiO₂ from SiCl₄+H₂O reveals the dependence of growth temperature on pK_a and on the steric bulk of the catalyst [76].

Because ALD depends on self-saturating surface reactions in the metal precursor pulse, it can be shown that the growth rate depends linearly on the degree to which ligands are eliminated during this pulse [18]. This motivates using the reaction energy for elimination [71] or the metal-ligand bond energy [82] as a simple metric for ALD growth rate (and perhaps even for the ALD growth temperature), allowing computational screening of a wide variety of ligands. Both of these screening studies investigate large, basic metal cations (La [71] and Sr [82]), where the steric demand of the

ligand must be balanced against its reactivity and the resulting trends agree well with experiment (*e.g.* unreactivity of β -diketonates). For this purpose, a cluster model is quick and efficient, as the influence of the surface is entirely neglected. The results agree well with experiment. In a similar vein, cluster models rationalize the elimination of protonated ligands from $\text{Ti}(\text{NMe}_2)_4$ *versus* $\text{Ti}(\text{O}^i\text{Pr})_4$ [93], from $\text{Zr}(\text{MeCp})_2(\text{Me})(\text{OMe})$ [107] and from $\text{Zr}(\text{Cp})_2(\text{Me})_2$ [110]. Such a simple approach is successful because ligand elimination (often termed ‘ligand exchange’) is known to be an important element of the mechanism of oxide ALD.

Another important element is revealed by Olivier *et al.*, who examine the tendency for Hf and Sn cations in oxide films to aggregate and increase their coordination number to oxygen, which they term ‘densification’ [70]. Based on this, the authors highlight the role of water as a co-reagent for oxide ALD, not only in providing reactive OH, but also in allowing densification via OH or O. Densification is important in ALD for the following reason. To be volatile, the metal centre in an ALD precursor molecule must be kept from aggregating with metal centers in neighboring molecules, which is achieved via the coordination of bulky ligands. By contrast, the product film should be a dense solid, with highly-coordinated metal atoms (bonded either to other metal atoms or to oxygen, sulfur *etc.*). As indicated in Equation 1 above, precursor adsorption and film growth therefore involves the change from low to high coordination of the constituent atoms. Zydor and Elliott have simulated the effect of ligand bulk in $\text{Ti}(\text{CpMe}_5)(\text{OMe})_3 + \text{H}_2\text{O}$, and thus explain the experimentally-observed lack of ALD as due to the inability of the hindered Ti centre to densify to the substrate [86], [87]. To date, the importance of densification as an element of ALD growth has not been widely recognized, although in hindsight, many of the published studies mentioned above show exothermic reactions correlating with increases in coordination number.

3.2. Mechanism of nitride ALD

Transition metal nitrides such as TiN and TaN are metallic and so of interest in thin film form as diffusion barriers. The first DFT study of nitride growth is by Tanaka *et al.*, computing $\text{TiCl}_4 + \text{NH}_3$ onto a cluster representing amorphous SiO_2 [88]; following adsorption, surface reactions between adsorbates via both the Langmuir–Hinshelwood and Eley–Rideal mechanisms were considered. In a

study of HfN growth from $\text{Hf}(\text{NMe}_2)_4 + \text{NH}_3$, it is found that the ALD mechanism is similar to that of HfO_2 from H_2O , although NH_3 is computed to be less reactive than H_2O and so O impurities could be a problem [68]. Thermal stability is a central question for transition metal amides/imides. The adsorption and decomposition of a whole sequence of such precursors shows that breaking metal-ligand bonds is the favoured pathway at low temperature, but also that C-H scission can lead to C impurities [69]. A comprehensive study of an amido/imido-Ta precursor with NH_3 shows that ammonia is a more facile source of N than the ligand, but also identifies decomposition pathways that may operate at elevated temperatures (MOCVD) [84]. Thermodynamic modeling of TaN is carried out using literature values [111].

In the growth of silicon nitride from $\text{SiH}_4 + \text{NH}_3$, the computed activation energies reveal why stoichiometric Si_3N_4 is favoured in ALD but a Si-rich material can be obtained in higher temperature CVD [79]. Boronitride growth has also been computed with DFT, although the radical intermediates that are postulated may be more relevant for CVD rather than ALD [41].

3.3. Mechanism of metal or elemental ALD

There is an extra layer of mechanistic complexity in the ALD of metals, since electrons must be transferred to metal cations during deposition in order to reduce them to the neutral product. Of the elementary steps that are known for oxide ALD, only reductive elimination is a candidate for showing how this might occur, and so there is a need for other redox reaction steps to be considered.

One of the earliest simulations of ALD is the investigation by Hirva and Pakkanen in 1989 of elemental silicon from silanes and chlorosilanes, in both radical and molecular mechanisms [78]. While chemisorption to bare Si surfaces is computed to be favourable, releasing HCl from the surface is more difficult. Although not a redox process, a related study by Mochizuki *et al.* considers GaAs growth from $\text{GaCl}_3 + \text{H}_2$ using high level *ab initio* methods [58]. The deposition of elemental carbon as diamond from fluorinated compounds is simulated by Hukka *et al.*, here focusing on radical pathways that may be more relevant for high-temperature CVD rather than ALD [43].

The *ab initio* simulation of metal ALD is pioneered in three papers by Mårtensson *et al.* that consider adsorption of Cu_2Cl_2 on a Cu (1 1 1) model surface [50], reaction with hydrogen [51] and barriers

[52]. Given the range of oxidation states available for Cu, disproportionation is one of the likely redox steps, but is computed here to be unfavourable for Cu(I)Cl. The Cl ligands are found to eliminate via combination with surface-H. The reduction potential of metals is emphasized in the method of Orimoto *et al.* for screening metal precursors, illustrated with DFT calculations on copper(II) β -diketonates that compare well with measured values [49]. DFT is also used for explicit calculation of the reaction energy and barrier for reducing a Ta(V) precursor with H radicals, as a model for TaCN growth with H₂/Ar plasma [83]. Care is needed in interpreting these results: because of the changing numbers of electrons in redox reactions, there is the possibility of poor error cancellation, leading to uncontrolled errors in the DFT energetics.

Substrate effects – nucleation, adhesion and island growth – are crucial in metal ALD. First principles dynamics give insights into Cu agglomeration and its temperature-dependence [112],[113]. Poor adhesion of Cu films is attributed to spontaneous precursor decomposition during adsorption onto metals, but not onto nitrides, based on the example of Cu(hfac)(vtms) on Ti, Ta and W [53],[54]. The adsorption of the same precursor onto Si is also computed and compared to experiments at a range of temperatures [55]. On a hydroxylated SiO₂ substrate, chemisorption of Cu₂(amd)₂ is shown to proceed by elimination of amdH, followed by release of amidine during the H₂ pulse, while transfer of ligands to the substrate can lead to contamination with C. These conclusions are reached via the powerful combination of DFT and *in situ* IR spectroscopy [48]. Co films are found to nucleate better from Co(^tBu-allyl)(CO)₃ on H-terminated Si rather than on OH-terminated SiO₂ substrates and this is rationalised via DFT energetics that show the Si-H surface to be a superior donor of H to the allyl group via Co, analogous with hydrosilylation catalysis [45].

Although not specific to ALD, a DFT study of the growth mode of Pt onto SrTiO₃ is also relevant [114]. There seem to be no DFT studies to date specifically devoted to noble metal ALD, despite the fact that open questions remain about the mechanism – perhaps this is because of the complexity of the redox mechanism relative to the Brønsted acid-base reactions of oxide ALD [115].

4. Simulating ALD onto silicon, silica and other substrates

Some of the most exciting applications of ALD are in the controlled deposition of sub-nanometre thin films onto a substrate, which we term ‘heterodeposition’ to distinguish it from the steady-state ‘homodeposition’ of section 3 above. For the electronics industry, the substrate is often a semiconductor, although the actual surface may be oxidised or cleaned, and there is also interest in ALD onto porous dielectrics and metal electrodes. Most non-electronics applications of ALD also depend on successful heterodeposition. If heterodeposition can be fully understood, it opens up the potential for interface control at the atomic level, which is particularly important if the target films are just a few nanometres thick. Of course, this level of understanding is still far off and relatively little is known at present about how ALD precursors interact with various substrates. Table 1 includes a summary of the atomic-scale simulations to date.

In terms of growth rate, heterodeposition has been classified as linear growth, inhibited growth or substrate-enhanced growth [116], followed by the transition to homodeposition or steady-state ALD. In the simplest case, substrate effects are limited to the earliest few ALD cycles, until a single monolayer of interfacial layer is formed, which is then followed by homodeposition. Detection of the interface reactions is only possible if *in situ* monitoring of adequate sensitivity is employed. The situation may be complicated if substrate and product mix to form a more extended inter-layer with its own distinct growth chemistry, as often the case when using an aggressive oxidising agent such as ozone. Alternatively, the product may homodeposit onto islands that ripen into a closed layer only after many ALD cycles.

One may envisage two chemical scenarios during heterodeposition. One possibility is that the same ALD mechanism operates as in homodeposition, modified only by the different coverage of reactive species (*e.g.* hydroxyl groups) on the substrate. Alternatively, non-ALD side-reactions may take place between precursor and substrate, either contributing extra product or etching the substrate away. First principles simulations clearly have a role to play in investigating what chemical interactions are possible between precursor and substrate. The situation is complicated by the strong dependence of heterodeposition on the preparation history of the substrate.

The (1 0 0) surface of diamond-structured silicon is the substrate used in the electronics industry, and a popular atomistic model is consequently the Si₉ cluster. This consists of an Si₂ surface dimer, on top of three (1 0 0)-oriented ‘layers’ of four+two+one Si atoms respectively. The subsurface layers are terminated with twelve H atoms, to give roughly tetrahedral Si coordination and no dangling bonds. The atoms of the surface dimer have one dangling bond each (if bare) or can be bound to H (simulating the situation after HF cleaning) or OH (after washing with H₂O). Tests indicate that activation energies from Si₉ are converged with respect to cluster size [20],[21], apparently due to the open structure of Si(1 0 0), since the same is not true for Si₁₀ as a model for more densely-packed Si(1 1 1) [20].

Modelling the ALD of elemental metals onto various substrates is outlined in section 3.3 above and the following sections concentrate on heterodeposition of compounds, mostly oxides.

4.1. Heterodeposition of zirconia and hafnia

Perhaps the earliest atomistic simulation of heterodeposition from two precursors is of B(OMe)₃ and POCl₃ onto silica [42]. However the most common subject is the ALD of high-*k* ZrO₂ or HfO₂ onto silicon-based substrates, because of its technological importance in nano-CMOS. Brodskii *et al.* use periodic and cluster models to compute the reactions of ZrCl₄ with hydroxylated silicon: elimination of HCl in the Zr-pulse is found to be endothermic, but subsequent hydrolysis of ZrCl₂ fragments in the H₂O pulse is slightly exothermic with a low activation barrier [102]. The adsorption of ZrCl₄ onto various substrates is compared: onto bare, H-terminated hydroxylated [97] and hydrated [98] Si surfaces and onto hydroxylated Ge [99]. A common theme is the tendency of the HCl by-product to remain complexed and not desorb [103],[104]. A similar pathway for the formation of a HCl intermediate from adsorbed HfCl₄ on Si(1 0 0) is computed by Estève [62] and on SiO₂ by Dkhissi *et al.* [63]. Slower kinetics are predicted when Si(OMe)₄ is introduced as co-precursor with HfCl₄ for hafnium silicate heterodeposition [80],[81].

Jeloica *et al.* compare three common precursors (AlMe₃, ZrCl₄ and HfCl₄) and find that they adsorb favourably on OH-terminated SiO₂, show similar barriers to H-transfer, but differ in ligand elimination energetics [22]. Calculations are presented for the same three precursors on GaAs,

showing the inhibiting effect of passivation with sulfur [23], and for HfCl_4 on hydroxylated GaAs [64]. Fenno *et al.* also compare Cl and Me ligands for ZrO_2 and HfO_2 heterodeposition, this time onto H-terminated Si, and also find CH_4 elimination to be much more favourable than HCl elimination [65]. Contamination with H_2O is predicted to lead to interfacial Si-O-Zr/Hf. Switching to amide ligands [67], decomposition reactions are computed to result in interfacial Si-C bonds [69], or Si-N and Si-CN bonds [11], which are important insights that can guide precursor choice for specific interface properties.

4.2. Heterodeposition of alumina

Halls and Raghavachari use DFT and the Si_9 model to reveal why AlMe_3 nucleates poorly on H-terminated Si: both adsorption and elimination of CH_4 are barely energetically favoured [25]. A side-reaction leading to O incorporation is identified and the reaction pathway is computed [26]. By contrast, if hydroxyl groups are present after treatment with H_2O , then both ALD half-reactions are computed to be thermodynamically favorable and kinetically uninhibited [27]. Indeed, many Lewis acidic metal precursors are found to adsorb favourably on OH-terminated SiO_2 and the Si-OH groups are sufficiently acidic for subsequent elimination [22]. Treatment with O_3 is shown to lead to Si-O-Al or Al-O- CH_3 but not SiO_2 [39]. Alternatively, a basic oxygen atom in the precursor [*e.g.* $\text{AlMe}_2(\text{O}^i\text{Pr})$] facilitates adsorption onto H-terminated Si [40]. More complex surface models are now becoming accessible to DFT calculations, as illustrated by a recent study of multiple AlMe_3 on Si-OH that shows an increase in activation energies as the surface becomes saturated [24].

For ALD of Al_2O_3 onto oxidised and clean Si_3N_4 , DFT calculations have been used to complement layer-by-layer experimental characterisation of the film, thus revealing when heterodeposition is inhibited/enhanced due to the availability of surface protons (standard ALD reactions) and when AlMe_3 is consuming the substrate (non-ALD reactions) [28]. These different modes of heterodeposition seem to affect the density and composition of the interfacial layer.

There is interest currently in replacing Si with higher mobility materials for the transistor channel and, consequently, the ALD of high-*k* dielectrics onto Ge, GaAs *etc.* is being studied. For AlMe_3 onto GaAs, Lu *et al.* compute adsorption and elimination reactions with hybrid DFT and find similar

energetic trends as on other OH-terminated surfaces [29]. Ren *et al.* find that these reactions become less favoured when GaAs is passivated with sulfur [23]. Surface structures of AlMe₃ fragments on InAs(0 0 1) and In_{0.53}Ga_{0.47}As(0 0 1) are computed with DFT and compared with scanning tunneling microscopy [30]. AlMe₃ can remove native oxides from GaAs surfaces and DFT calculations point out the role of Ga-OH vs As-O in this process, as well as proposing a redox reaction [117]. Klejna and Elliott extend this to computing seven possible reaction pathways and find that arsenic oxides are predominantly reduced to gaseous As₄ gas and solid GaAs, with C lost as C₂H₆ [31]. This illustrates that AlMe₃ is a multi-purpose reagent for surface preparation, functioning as a Lewis acid (due to under-saturated Al), as a Brønsted base (CH₃⁻ to CH₄) and also as a reducing agent (CH₃⁺ plus two electrons). DFT thus reveals that the mechanistic step of reduction takes place when CH₃ migrates from surface-bound Al/As/Ga to O [31].

Adsorption of AlMe₃ onto H-terminated Ge is found to be more favourable than that onto Si-H, but still hindered, when compared with OH-terminated Si [32],[33]. Using Ge-SH as a model for sulfur-passivated Ge, DFT shows favourable adsorption of AlMe₃ and no removal of S [21].

Moving to C-based substrates, the ALD of Al₂O₃ onto the open edges of a graphene nanoribbon is studied with DFT for a range of temperatures and pressures, revealing selectivity for the zigzag edge during the H₂O pulse [34]. For organic molecules, Al₂O₃ ALD onto self-assembled monolayers (SAMs) is computed to be favourable in terms of adsorption and elimination on amine- and hydroxyl-terminations, but not on methyl-terminated molecules [35].

4.3. Heterodeposition of titanium-based materials

Titanium oxides and nitrides are important materials and their heterodeposition onto silicon-based substrates can easily be studied by extension of the models for hafnia and zirconia. Hu *et al.* investigate TiCl₄+H₂O ALD onto various models of the SiO₂ surface and find a strong dependence of the growth rate and morphology on coverage and arrangement of reactive groups [91]. This is contrasted with the TiI₄+H₂O process, where binding energies are computed to be higher and impurity levels to be lower [92]. On H-terminated Si, direct chlorination is found to be the kinetically favoured

reaction of TiCl_4 [90]. High-temperature reactions of a Ti(III) precursor with SiO_2 are also computed with DFT and found to agree with solid-state NMR [85].

An early study of the adsorption of NH_3 onto bare Si [74] is followed with simulation of reaction steps for heterodeposition of TiN on SiO_2 from $\text{TiCl}_4 + \text{NH}_3$ [88]. DFT simulations and IR spectra are integrated in a substantial study of TiN onto silicon from $\text{Ti}(\text{NMe}_2)_4$ by Rodriguez-Reyes *et al.*, investigating also amides of other transition metals.[69] The precursor is proposed to adsorb onto bare Si via N and then undergo N-Ti scission, based on a lower barrier relative to N-C scission [94]. This leads in turn to weakening of C-H, which is consistent with data from temperature-programmed desorption [95]. Several decomposition pathways are computed to lead to Si-C bonds, explaining the high carbon content at the interface. On an ammonia-saturated surface, the dominant reaction is found to be transamination, which again matches IR results [7].

Like heterodeposition onto Si, ALD onto SAMs also depends on their chemical termination. Amidotitanium precursors are computed to form adducts with amine-terminated SAMs, but H-bonds with thiol- or hydroxyl-terminated SAMs, while the amidozirconium analogues always form dative-bonded adducts [108].

4.4. Heterodeposition of other oxides and sulfides

The pyridine-catalysed deposition of SiO_2 from an alternating sequence of $\text{SiCl}_4 + \text{H}_2\text{O}$ on a Si substrate is computed using MP2, which is a post-HF *ab initio* method for improved description of van der Waals forces [77]. Kang *et al.* consider the same system without catalysis using DFT and find that the standard mechanistic steps occur in both half-cycles: adsorption, elimination of HCl and movement to bridging sites [8]. The overall barrier matches the experimental value remarkably well. Reaction and activation energies for ALD steps onto hydroxylated Si are also computed for ZnO from $\text{Zn}(\text{C}_2\text{H}_5)_2 + \text{H}_2\text{O}$ [96], Y_2O_3 from $\text{Y}(\text{C}_5\text{H}_5)_3 + \text{H}_2\text{O}$ [109], and MgO from $\text{Mg}(\text{C}_5\text{H}_5)_2 + \text{H}_2\text{O}$ [72]. PbS growth is shown with DFT to be unfavourable on a methyl-terminated SAM, so that ALD takes place selectively on the areas not covered with SAM [75].

Simulations are now increasingly being reported of the mechanism of oxide ALD onto more complex substrates. Popovici *et al.* compute that HfCl_4 reactivity is enhanced on a Ti-OH substrate while

depositing hafnium titanate [59]. For hafnium aluminate, Nyns *et al.* use DFT calculations to show that changes relative to the respective binary oxides are due to different dehydroxylation behaviour of the ternary substrate [36]. The reactive adsorption of AlMe_3 onto anatase- TiO_2 surfaces is shown with DFT to produce atomically rough films [16] and to proceed only at defects and edges where water is adsorbed, explaining the experimentally-observed island growth [37].

5. Thermal stability of ALD precursors

The study of ALD must also include the study of low-temperature or surface-catalysed CVD. CVD reactions are generally responsible for an upper limit to the ALD temperature window and associated impurity levels in homodeposition, [84] and can explain heterodeposition by certain precursors and resulting interfaces with substrates [7],[11],[69],[53],[54],[94],[95]. New ALD precursors should be designed so as to be thermally stable, minimising unwanted CVD-like decomposition during storage and delivery of the precursor. As shown by the examples below, this is an area where *ab initio* simulation can contribute, although finding unknown decomposition reactions is much harder than confirming a known ALD mechanism.

A DFT assessment of decomposition reactions of various amido/imido Mo precursors reveal why the di-isopropylamido complex is the least stable, as determined by calorimetry [73]. Calculations by Zydor and Elliott show that intramolecular α -H transfer in Zr and Hf precursors $\text{M}(\text{MeCp})_2(\text{Me})_2$ accounts for experimentally-observed decomposition and can be avoided by altering the ligands or increasing the electrophilicity of the metal [106]. The effect on electrophilicity is also calculated for related precursors with bridged cyclopentadienyl ligands [66]. Using DFT corrected for dispersion, the fragmentation modes of a Cu(I) guanidinate precursor are computed by Coyle *et al.* to be carbodiimide deinsertion and β -H elimination, with the latter pathway agreeing with results from mass spectrometry and IR spectroscopy [56]. Migration of β -H is also the focus of a first principles study of Co and Ni amidinate precursors, giving relative stabilities in agreement with experiment [46],[47].

6. Conclusion and outlook

The main aspects of ALD chemistry that have been addressed by first principles atomic-scale modelling are growth reactions, substrate effects and precursor decomposition. A wider range of issues, such as growth rate, film uniformity and reactor design, can be addressed by ‘multi-scale modelling’, *i.e.* using the atomistic results as inputs to other scales of simulation. Nevertheless, many ambitious targets remain; for instance, there are no models to date that explicitly show how precursor chemistry and reactor conditions dictate nanomorphology. Predicting precursor volatility is another open question for simulation.

Simulations have mostly addressed the ALD of oxides and nitrides, with relatively little on metals and chalcogenides. By far the most common subject to date has been computing reaction steps in the deposition of high-*k* dielectrics (HfO_2 , ZrO_2 , Al_2O_3) onto silicon-based substrates, clearly driven by the interest from the semiconductor industry that has propelled ALD into prominence over this period. A few simulations have considered inorganic ALD onto organic molecules, but there has been no modeling yet of the issues unique to molecular layer deposition.

For mechanistic questions, density functional theory (DFT) is the method of choice and this is mostly used to compute reaction and activation energies for adsorption and ligand elimination from a single precursor molecule interacting with an idealised reactive surface. The simulations reveal a palette of competing reactions, subject to fascinating stereochemical effects. Recently, more attention is being paid to interactions between adsorbate fragments on the surface, leading to steps such as densification that can have a major influence on growth. Detailed models of non-ALD decomposition reactions during heterodeposition onto various substrates are also emerging, opening up the potential for using ALD precursors to achieve atom-by-atom control of interfaces. Nevertheless, an open challenge is the reliable simulation of redox reactions and plasma-based ALD processes.

One of the strengths of DFT and other first principles approaches is that quantitative data (such as reaction energetics) can be obtained without fitting to experiment. However, whether a single reaction step is endothermic or exothermic is not in itself evidence of whether it plays a role in deposition. Only a series of simulations provide useful insights – *e.g.* assessing which decomposition reaction is most likely – and so the choice of model and its interpretation remains the greatest source

of uncertainty. First principles results have turned out to be most powerful when they can add atomic-scale explanation to experimental data, particularly *in situ* techniques such as IR spectroscopy. More generally, simulations must aim to move beyond simply validating data already available from experiment, and instead explain, predict and contribute to innovations in ALD processing.

Acknowledgements

Financial support from Science Foundation Ireland under “ALDesign”, 09.IN1.I2628, and assistance from Ms T. Harte in preparing the manuscript is gratefully acknowledged.

References

- [1] Jonsson H 2000 *Annual Review of Physical Chemistry* **51** 623-53
- [2] Sautet P, Delbecq F 2010 *Chemical Reviews* **110** 1788-806
- [3] Hafner J 2000 *Acta Materialia* **48** 71-92
- [4] Kohn W, Becke A D, Parr R G 1996 *The Journal of Physical Chemistry* **100** 12974-80
- [5] Zhao Y, Truhlar D G 2008 *Accounts of Chemical Research* **41** 157-67
- [6] Kwon J, Dai M, Halls M D, Langereis E, Chabal Y J, Gordon R G 2009 *Journal of Physical Chemistry C* **113** 654-60
- [7] Rodriguez-Reyes J C F, Teplyakov A V 2007 *Journal of Physical Chemistry C* **111** 16498-505
- [8] Kang J K, Musgrave C B 2002 *Journal of Applied Physics* **91** 3408
- [9] John A. T. Norman, Melanie Perez, M. S. Kim, Xinjian Lei, Sergei Ivanov, Agnes Derecskei-Kovacs, et al. 2011 *Inorganic Chemistry* **50**(24) 12396–8
- [10] Siodmiak M, Frenking G, Korkin A 2000 *Journal of Physical Chemistry A* **104** 1186-95
- [11] Li K, Li S, Li N, Dixon D A, Klein T M 2010 *Journal of Physical Chemistry C* **114** 14061-75
- [12] Heyman A, Musgrave C B 2004 *The Journal of Physical Chemistry B* **108** 5718-25
- [13] Mukhopadhyay A, Musgrave C 2006 *Chemical Physics Letters* **421** 215-20
- [14] Widjaja Y, Musgrave C B 2002 *Applied Physics Letters* **80** 3304
- [15] Elliott S D, Greer J C 2004 *Journal of Materials Chemistry* **14** 3246
- [16] Mäkinen V, Honkala K, Häkkinen H 2011 *Journal of Physical Chemistry C* **115** 9250-9
- [17] Xu; K, Ye P D 2010 *J. Phys. Chem. C* **114** 10505-11
- [18] Elliott S D 2005 *Computational Materials Science* **33** 20-5
- [19] Shankar S, Simka H, Haverty M 2008 *Journal of Physics: Condensed Matter* **20** 064232
- [20] Halls M D, Raghavachari K 2004 *Journal of Physical Chemistry A* **108** 2982-7
- [21] Delabie A, Sioncke S, Rip J, Van Elshocht S, Caymax M, Pourtois G, et al. 2011 *Journal of Physical Chemistry C* **115**(35) 17523–32
- [22] Jeloica L, Estève A, Djafari Rouhani M, Estève D 2003 *Applied Physics Letters* **83** 542
- [23] Ren J, Zhou G, Hu Y, Jiang H, Zhang D 2008 *Applied Surface Science* **254** 7115-21
- [24] Kim D-H, Baek S-B, Seo H-I, Kim Y-C 2011 *Applied Surface Science* **257** 6326-31
- [25] Halls M D, Raghavachari K 2003 *Journal of Chemical Physics* **118** 10221
- [26] Halls M, Raghavachari K, Frank M, Chabal Y 2003 *Physical Review B* **68** 161302
- [27] Halls M D, Raghavachari K 2004 *Journal of Physical Chemistry B* **108** 4058-62
- [28] Lamagna L, Wiemer C, Perego M, Spiga S, Rodriguez J, Coll D S, et al. 2012 *Chemistry of Materials* **24**(6) 1080-90

- [29] Lu H-L, Chen W, Ding S-J, Xu M, Zhang D W, Wang L-K 2005 *Journal of Physics: Condensed Matter* **17** 7517-22
- [30] Clemens J B, Chagarov E A, Holland M, Droopad R, Shen J, Kummel A C 2010 *Journal of Chemical Physics* **133** 154704
- [31] Klejna S, Elliott S D 2012 *Journal of Physical Chemistry C* **116** 643-54
- [32] Yu S, Qing-Qing S, Lin D, Han L, Shi-Jin D, Wei Z 2009 *Chinese Physics Letters* **26** 053101
- [33] Shi Y, Sun Q-Q, Dong L, Liu H, Ding S-J, Zhang W 2009 *Chinese Physics Letters* **26** 053101
- [34] Xu K, Ye P D 2010 *J. Phys. Chem. C* **114** 10505-11
- [35] Xu Y, Musgrave C B 2004 *Chemistry of Materials* **16** 646-53
- [36] Nyns L, Delabie A, Pourtois G, Van Elshocht S, Vinckier C, De Gendt S 2010 *Journal of The Electrochemical Society* **157** G7-G12
- [37] Terranova U, Bowler D R 2011 *Journal of Materials Chemistry* **21** 4197
- [38] Elliott S D, Scarel G, Wiemer C, Fanciulli M, Pavia G 2006 *Chemistry of Materials* **18** 3764-73
- [39] Kwon J, Dai M, Halls M D, Chabal Y J 2008 *Chemistry of Materials* **20** 3248-50
- [40] Ghosh M K, Choi C H 2006 *Journal of Physical Chemistry B* **110** 11277-83
- [41] Arvidsson I, Larsson K 2007 *Diamond and Related Materials* **16** 131-7
- [42] Gun'ko V M 1993 *Kinetika i Kataliz* **34** 463-6
- [43] Hukka T 1996 *Surface Science* **359** 213-26
- [44] Tanskanen J T, Bakke J R, Bent S F, Pakkanen T A 2010 *Journal of Physical Chemistry C* **114** 16618-24
- [45] Jinhee Kwon, Mark Saly, Mathew D. Halls, Ravindra K. Kanjolia, Chabal Y J 2012 *Chemistry of Materials* **24**(6) 1025-30
- [46] Li J, Wu J, Zhou C, Han B, Lei X, Gordon R, et al. 2009 *International Journal of Quantum Chemistry* **109** 756-63
- [47] Li J-Y; Wu, Jin-Ping; Zhou, Cheng-Gang; Yao, Shu-Juan; Han, Bo 2008 *Acta Chimica Sinica* **66** 165-9
- [48] Dai M, Kwon J, Halls M D, Gordon R G, Chabal Y J 2010 *Langmuir* **26** 3911-7
- [49] Orimoto Y, Toyota A, Furuya T, Nakamura H, Uehara M 2009 *Industrial & Engineering Chemistry Research* **48**(7) 3389-97
- [50] Mårtensson P 1998 *Applied Surface Science* **136** 137-46
- [51] Mårtensson P 1999 *Applied Surface Science* **148** 9-16
- [52] Mårtensson P 2000 *Applied Surface Science* **157** 92-100
- [53] Machado E, Kaczmariski M, Braida B, Ordejón P, Garg D, Norman J, et al. 2007 *Journal of Molecular Modeling* **13** 861-4
- [54] Machado E, Kaczmariski M, Ordejón P, Garg D, Norman J, Cheng H 2005 *Langmuir* **21** 7608-14
- [55] Pirolli L, Teplyakov A V 2006 *Surface Science* **600** 3313-20
- [56] Coyle J P, Johnson P A, DiLabio G A, Barry S T, Müller J 2010 *Inorganic chemistry* **49** 2844-50
- [57] Nolan M, Elliott S D 2010 *Chemistry of Materials* **22** 117-29
- [58] Mochizuki Y, Takada T, Usui A 1994 *Applied Surface Science* **82-83** 200-7
- [59] Popovici M, Delabie A, Van Elshocht S, Clima S, Pourtois G, Nyns L, et al. 2009 *Journal of The Electrochemical Society* **156** G145-G51
- [60] Widjaja Y, Musgrave C B 2002 *Journal of Chemical Physics* **117** 1931
- [61] Mukhopadhyay A B, Musgrave C B, Sanz J F 2008 *Journal of the American Chemical Society* **130** 11996-2006
- [62] Estève A 2003 *Computational Materials Science* **27** 75-80

- [63] Dkhissi A, Mazaleyrat G, Estève A, Djafari Rouhani M 2009 *Physical Chemistry Chemical Physics* **11** 3701
- [64] Lu H-L, Xu M, Ding S-J, Chen W, Zhang D W, Wang L-K 2006 *Applied Physics Letters* **89** 162905
- [65] Fenno R D, Halls M D, Raghavachari K 2005 *Journal of Physical Chemistry B* **109** 4969-76
- [66] Black K, Aspinall H C, Jones A C, Przybylak K, Bacsa J, Chalker P R, et al. 2008 *Journal of Materials Chemistry* **18** 4561
- [67] Kim D-H, Kim D-H, Seo H-I, Kim Y-C 2011 *Journal of Nanoscience and Nanotechnology* **11**(5) 4324-7
- [68] Xu Y, Musgrave C 2005 *Chemical Physics Letters* **407** 272-5
- [69] Rodríguez-Reyes J C F, Teplyakov A V 2008 *Journal of Applied Physics* **104** 084907
- [70] Olivier S, Ducéré J-M, Mastail C, Landa G, Estève A, Rouhani M D 2008 *Chemistry of Materials* **20** 1555-60
- [71] Elliott S D 2007 *Surface and Coatings Technology* **201** 9076-81
- [72] Lu H-L, Ding S-J, Zhang D W 2009 *Journal of Physical Chemistry A* **113** 8791-4
- [73] Miiikkulainen V, Suvanto M, Pakkanen T A 2008 *Chemical Vapor Deposition* **14** 71-7
- [74] Widjaja Y, Mysinger M M, Musgrave C B 2000 *Journal of Physical Chemistry B* **104** 2527-33
- [75] Lee W, Dasgupta N P, Trejo O, Lee J-R, Hwang J, Usui T, et al. 2010 *Langmuir* **26** 6845-52
- [76] Chen S, Fang G, Qian X, Li A, Ma J 2011 *Journal of Physical Chemistry C* **115**(47) 23363-73
- [77] Okamoto Y 1999 *Journal of Physical Chemistry B* **103** 11074-7
- [78] Hirva P, Pakkanen T 1989 *Surface Science* **220** 137-51
- [79] Mui C 2004 *Surface Science* **557** 159-70
- [80] Ren J, Zhang Y-T, Zhang D W 2007 *Journal of Molecular Structure: THEOCHEM* **803** 23-8
- [81] Ren J, Hu Y, Wang J, Jiang H, Zhang D 2008 *Thin Solid Films* **516** 2966-72
- [82] Timothy P. Holme, Prinz F B 2007 *Journal of Physical Chemistry A* **111**(33) 8147-51
- [83] Xie Q, Deduytsche D, Musschoot J, Meirhaeghe R L V, Detavernier C, Ding S-F, et al. 2011 *Microelectronic Engineering* **88** 646-50
- [84] Somani S, Mukhopadhyay A, Musgrave C 2011 *Journal of Physical Chemistry C* **115** 11507-13
- [85] Wasslen Y A, Tois E, Haukka S, Kreisel K A, Yap G P A, Halls M D, et al. 2010 *Inorganic Chemistry* **49** 1976-82
- [86] Zydor A, Elliott S D 2011 *Journal of Nanoscience and Nanotechnology* **11** 8089-93
- [87] Zydor A, Kessler V G, Elliott S D 2012 *Phys. Chem. Chem. Phys.*
- [88] Tanaka T 2002 *Thin Solid Films* **409** 51-7
- [89] Ghosh M K, Choi C H 2008 *Chemical Physics Letters* **457** 69-73
- [90] Ghosh M K, Choi C H 2008 *Chemical Physics Letters* **461** 249-53
- [91] Hu Z, Turner C H 2006 *Journal of Physical Chemistry B* **110** 8337-47
- [92] Hu Z, Turner C H 2007 *Journal of the American Chemical Society* **129** 3863-78
- [93] Xie Q, Jiang Y-L, Detavernier C, Deduytsche D, Van Meirhaeghe R L, Ru G-P, et al. 2007 *Journal of Applied Physics* **102** 083521
- [94] Rodríguez-Reyes J C F, Teplyakov A V 2007 *Journal of Physical Chemistry C* **111** 4800-8
- [95] Rodríguez-Reyes J C F, Teplyakov A V 2008 *Journal of Physical Chemistry C* **112** 9695-705
- [96] Ren J 2009 *Applied Surface Science* **255** 5742-5

- [97] Widjaja Y, Han J H, Musgrave C B 2003 *Journal of Physical Chemistry B* **107** 9319-24
- [98] Petersen M 2004 *Computational Materials Science* **30** 77-80
- [99] Chen W, Zhang D, Ren J, Lu H, Zhang J, Xu M, et al. 2005 *Thin Solid Films* **479** 73-6
- [100] Deminsky M 2004 *Surface Science* **549** 67-86
- [101] Mukhopadhyay A B, Sanz J F, Musgrave C B 2006 *Chemistry of Materials* **18** 3397-403
- [102] Brodskii V, Rykova E, Bagatur'yants A, Korkin A 2002 *Computational Materials Science* **24** 278-83
- [103] Han J H, Gao G, Widjaja Y, Garfunkel E, Musgrave C B 2004 *Surface Science* **550** 199-212
- [104] Jeloica L, Esteve A, Dkhissi A, Esteve D, Djafari Rouhani M 2005 *Computational Materials Science* **33** 59-65
- [105] Jie Ren C C, Guangfen Zhou, Yanchun Liu, Yongqi Hu, Baozhu Wang, Hu, Yongqi 2011 *Thin Solid Films* **519** 3716-21
- [106] Zydor A, Elliott S D 2010 *Journal of Physical Chemistry A* **114** 1879-86
- [107] Elam J W, Pellin M J, Elliott S D, Zydor A, Faia M C, Hupp J T 2007 *Applied Physics Letters* **91** 253123
- [108] Haran M, Engstrom J R, Clancy P 2006 *Journal of the American Chemical Society* **128** 836-47
- [109] Ren J, Zhou G, Hu Y, Zhang D W 2009 *Applied Surface Science* **255** 7136-41
- [110] Ren J, Cui C, Zhou G, Liu Y, Hu Y, Wang B 2011 *Thin Solid Films* **519** 3716-21
- [111] Blanquet E, Nuta I, Brizé V, Boichot R I, Mantoux A, Violet P, et al., editors. (Invited) Developments of ALD Processes: Experiments and Thermodynamic Evaluations. ECS Transactions; 2010.
- [112] Han B, Wu J, Zhou C, Li J, Lei X, Norman J A T, et al. 2008 *The Journal of Physical Chemistry C* **112** 9798-802
- [113] Wu J, Han B, Zhou C, Lei X, Gaffney T R, Norman J A T, et al. 2007 *Journal of Physical Chemistry C* **111** 9403-6
- [114] Asthagiri A, Sholl D S 2002 *Journal of Chemical Physics* **116** 9914
- [115] Elliott S D 2010 *Langmuir* **26** 9179-82
- [116] Puurunen R L 2005 *Journal of Applied Physics* **97** 121301
- [117] Hegde G, Klimeck G, Strachan A 2011 *Applied Physics Letters* **99** 093508